IG-CVAE: A Multi-Modality Framework for Deciphering Alzheimer's Disease Through MRI and Synthetic Gene Expression Data

1st Xiaoqing Huang
Biostatistics and Health Data Science
Indiana University Indianapolis
Indianapolis, USA
huanxi@iu.edu

1st Ronak Laxmanbhai Bhagchandani
Computer Science Department
Indiana University Bloomington
Bloomington, USA
rbhagcha@iu.edu

2nd Rishit Puri
Computer Science Department
Indiana University Bloomington
Bloomington, USA
rispuri@iu.edu

3rd Nischal Bangalore Krupashankar
Computer Science Department
Indiana University Bloomington
Bloomington, USA

4th Dilip Nikhil Francies
Computer Science Department
Indiana University Bloomington
Bloomington, USA

5th Mu Zhou
Computer Science Department
Rutgers University
Piscataway, USA

6th Kun Huang
Biostatistics and Health Data Science
Indiana University Indianapolis
Indianapolis, USA

7th Jie Zhang
Department of Medical and Molecular Genetics
Indiana University Indianapolis
Indianapolis, USA

8th Yijie Wang
Computer Science Department
Indiana University Bloomington
Bloomington, USA

***Abstract*—Alzheimer's disease (AD) is one of the leading causes of dementia worldwide. Multimodal datasets have immense potential to detect and characterize AD with high precision and at an earlier age. However, the limited availability of genetic and neuroimaging paired data poses a significant barrier in ADNI and ANMerge dataset, constraining the ability to fully capture the molecular complexities and heterogeneity of the disease. Methods: This study proposes a novel deep learning approach to generate gene expression feature vector data from 3D MRI using conditional variational autoencoders (CVAE) with Gaussian distribution from ADNI and ANMerge, named image genetic CVAE (IG-CVAE), where IG-CVAE generates gene feature vector with novel loss functions - IG-CVAE Loss. Results: IG-CVAE achieved a mean squared error (MSE) of 0.217, mean absolute error (MAE) of 0.217, mean absolute percentage error (MAPE) of 1.43, and a cosine similarity of 0.99997 on ADNI dataset. The feature vectors generated by the 3D MRI model, along with the classification layer, achieved an accuracy of 82% in predicting the state of AD or cognitively normal (CN), and the final layer feature vectors are used as input for IG-CVAE. The gene expression feature vectors along with the classification layer, achieved an accuracy of 85% in predicting AD or CN status, and the final layer feature vectors are used to compare and train IG-CVAE model. The generated feature vector through IG-CVAE and undiscovered gene expression data is used to train a MLP model with total 500 patients to predict AD/CN achieved an accuracy of 84% with a precision of 96%. We further validate the model using the ANMerge dataset where the IG-CVAE model generates feature vector with an MSE of 0.08, MAE of 0.106 and cosine similarity of 0.99998. The generated feature vector with total 500 patients were trained on MLP model to predict AD/CN received an accuracy of 96%. Discussion: Using IG-CVAE, we can generate synthetic gene expression feature vector data directly from MRI scans, dramatically increasing both the availability and quality of gene expression feature vector data which enhance the prediction of AD. This approach can potentially enhance early detection and deepen our understanding of AD, ultimately driving more precise diagnostics and targeted therapeutic strategies.**

***Index Terms*—Conditional Variational Autoencoder (CVAE), Gene Expression Data, MRI Data Analysis, Gene-MRI Relationship Mapping, Precision Medicine.**

We gratefully acknowledge the funding received for this work from the Indiana University Precision Health Initiative National Institutes of Health (NIH) TREAT-AD U54 grant 5U54AG065181, 5R01NS119280, and R35GM147241 to Y.W. This research was supported in part by Indiana University Faculty Assistance in Data Science Program and Lilly Endowment, Inc., through its support for the Indiana University Pervasive Technology Institute. All theses supports have been essential in facilitating our research endeavors.

I. Introduction

The most common type of dementia, AD, affects millions of people worldwide and presents significant problems for healthcare systems because of its progressive and deteriorating character [1]. The clinical diagnosis of AD typically relies on clinical assessments, cognitive testing, neuroimaging techniques, and biomarker tests, including genetic profiling. Despite these advances, the disease's complexity, characterized by heterogeneity and symptom overlap with other co-existing dementia types, such as vascular dementia and Lewy body dementia complicates accurate diagnosis [2]. A more focused exploration of image and gene biomarkers may provide significant advancements in early and accurate detection.

Researchers now have strong tools to better understand the underlying mechanisms of AD, thanks to recent developments

in neuroimaging and genetics [3]. Finding genetic variations linked to the risk and development of AD has been made possible in large part by genome-wide association studies (GWAS) [4]. For instance, a GWAS focusing on brain connectivity changes identified key genes such as ANTXR2, IGF1, and JAK1 that are implicated in the disease [5]. These genetic markers offer critical insights into the biological processes that drive AD, complementing the structural and functional information provided by neuroimaging modalities like magnetic resonance imaging (MRI) and positron emission tomography (PET). The integration of multiple data types, especially the combination of genomic data with neuro-imaging, is becoming increasingly important in AD research [5][6]. Integrative models, such as those combining transcriptomics, genomics, and imaging data, have shown promise in improving the accuracy of AD classification. For example, federated learning models have been developed to integrate genotype, gene expression, and imaging data, facilitating a more personalized understanding of AD while preserving data privacy across institutions [7]. Despite these advances, a significant challenge remains the limited availability of genetic data associated with neuroimaging at the patient visit level, which is essential for understanding the molecular basis of AD [8]. While neuroimaging provides detailed structural information, it lacks the molecular specificity that genetic data can offer, and this limitation has hindered the development of more robust predictive models that can accurately classify individuals as suffering from AD or CN. To address this gap, previous research has explored various methods to generate or infer missing data in multi-modality datasets. Approaches like the Disease-Image-Specific Deep Learning (DSDL) framework have been developed to synthesize missing neuroimaging data, helping to complete datasets and improve disease classification [9]. However, although these methods successfully generate data that are structurally consistent with existing imaging methods, they often fail to produce biologically meaningful data, especially when synthesizing gene expression profiles. This limitation is crucial because gene expression data encapsulate the active transcriptional landscape of cells and provide insight into the molecular basis of AD that cannot be captured by imaging data alone. Several other studies have attempted integrating different omics data, such as methylation or proteomics, with neuroimaging to create a more comprehensive view of AD [10][11][12][13]. However, these methods face significant challenges due to the static nature of genomic and epigenomic data, which do not capture the dynamic and context-dependent gene expression changes that occur during disease progression. Gene expression data, in contrast, offers a dynamic snapshot of cellular activity, reflecting the immediate molecular responses to pathological changes in the brain. This makes gene expression a particularly powerful tool for understanding AD at the molecular level [14]. By focusing on gene expression in combination with neuroimaging, we can correlate transcriptional changes with structural and functional changes in the brain, providing a more holistic view of disease onset and progression. Although the abundance of gene expression data in AD research, the problem lies in where we want to use multi modality for the same patient like the limited availability of datasets where both gene expression and neuroimaging data are available for the same patients for the same year. This scarcity hinders the development of integrative models that can fully exploit the complementary strengths of these modalities.

Recognizing this gap, we propose a novel approach called image-genetic conditional variational autoencoders with Gaussian distribution (IG-CVAE) that leverages conditional variational autoencoders to generate gene expression feature vector data from 3D MRI features. The IG-CVAE model is enhanced with cosine similarity loss, which together ensures that the generated gene expression feature vector data not only statistically aligns with actual feature vector data but also maintains its biological relevance—revealing key molecular signatures that are essential for accurate disease classification. By generating gene expression feature vector data that is consistent with existing MRI features, our method offers a valuable tool for researchers seeking to better understand the molecular mechanisms underlying AD etiology and heterogeneity and improve the accuracy of AD versus CN classification models at an earlier stage using generated gene expression data from MRI scans. This work builds on the successes of integrative models in the field, introducing a more sophisticated approach to data generation that specifically targets the challenges of data scarcity issues in multi-modality integration in AD research.

II. Methods

A. Data Sources

This study utilizes the Alzheimer's Disease Neuroimaging Initiative (ADNI) datasets, specifically the ADNIGO and ADNI2 phases, along with ANMerge dataset[15], providing 3D MRI and gene expression data for the same patients at the same visits within the same year. As the datasets consists of comprehensive collection of neuroimaging and molecular data, making them ideal for our study. The inclusion of the ANMerge dataset enhances the scope of the analysis by incorporating additional harmonized molecular and imaging data, further improving the reliability of the findings. The 3D MRI data includes T1-weighted structural scans, which are preprocessed using standard neuroimaging pipelines to ensure consistency across samples [16].

The gene expression data derived from blood samples is limited in quantity but essential for understanding the molecular underpinnings of AD. We carefully curated this data to ensure that it matches the corresponding MRI scans, which allows for meaningful correlations between the imaging and genetic modalities by combining diagnosis data and MRI metadata information based on year and subject ID into consideration. To enhance the model performance of the gene expression data, we performed differential gene expression analysis using the limma package in R [17]. This analysis identifies genes that show significant differences in expression between AD patients and cognitively normal controls. From

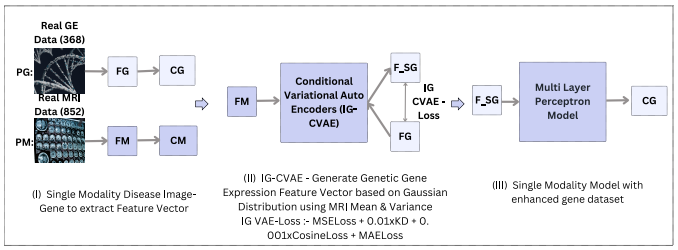

Fig. 1. Illustration of our IG-CVAE Model. Two major components included are: (I) Trained two single modality disease-specific neural networks for classification and learning disease image-gene specificity for GE (i.e. $PG = FG + CG$) and MRI (i.e. $PM = FM + CM$) and (II) a Conditional Auto Encoders to fill missing Gene Expression feature vector data generated from MRI Data with IG-CVAE Loss. (III) Trained a MLP model to predict whether a patient has AD or CN with synthetic feature vector data generated from II. Note FM and FG are learned in (I) and kept frozen in (II). Note: PG: gene expression model; FG: feature extraction layer; $CG : AD/CN$ Classification layer for gene expression data; PM: MRI model; FM: feature extraction layer for MRI Data; $CM : AD/CN$ classification layer for MRI data; F_SG: synthetic gene expression feature vector generated from MRI model.

this analysis, we selected the top 1,000 gene symbols based on their average weighted p-values, and further refine our dataset, we selected the top 464 gene symbols based on their absolute log fold change (logFC) values greater than 0.04 in ADNI and ANMerge dataset, a screening threshold balance the magnitude and significance, which are then used as the most highly variable genes for the generative model. In ADNI there are 368 patients with combined gene expression data and MRI data, where 248 patients have been diagnosed as CN and 120 as having AD. These data are only available in the ADNIGO and ADNI-2 phases of the ADNI study, and both datasets are measured in the same year. For the MRI data, we have a total of 852 scans and for gene expression data we have a total of 368 scans across 368 patients. Each patient, identified by their subject ID, may have multiple MRI scans, but all scans are taken during the same year and share the same diagnosis.

While in ANMerge dataset there are 266 patients with combined gene expression data and MRI data, where 196 patients have been diagnosed as AD and 70 as having CN. Gene Expression data are only available in the Month of 0-3 while MRI dataset is available in the Month of 0-6, 12-24.

B. Model Architecture

Our proposed IG-CVAE model has two components. First, train gene expression branch and MRI branch to individually and extract feature vectors. Second, use MRI feature vector to generate gene expression feature vector using the CVAE model and compare the results with the gene feature vector obtained from the first step. The entire pipeline was implemented using Python 3.11.8 and PyTorch, with computational tasks performed on the Quartz supercomputing infrastructure. Hyperparameter tuning was conducted using Optuna, an optimization framework, to efficiently explore and select the best model parameters. The model training, optimized on Quartz's GPU resources.

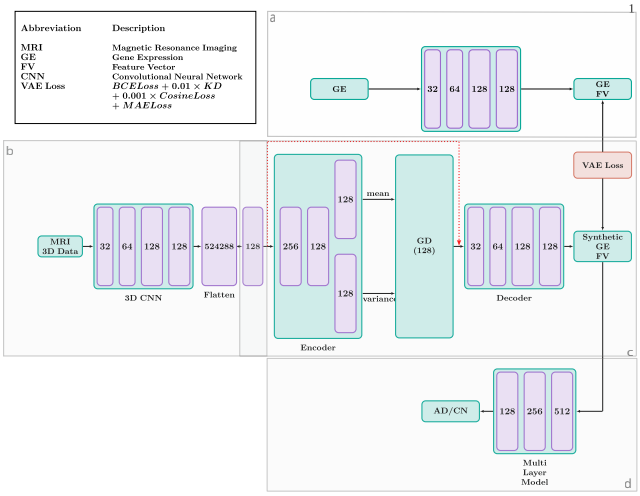

Fig. 2. Illustration of our proposed IG-CVAE model. Four major components are added: (a) Training the gene expression model with ADNI Gene Expression data to extract feature vectors from gene data; (b) Training the MRI model with ADNI MRI Dataset to extract feature vectors from MRI data; (c) Utilizing the MRI feature vectors as input to the Conditional Variational Autoencoder (CVAE) model, which generates corresponding gene expression feature vectors guided by the IG-CVAE loss; (d) Using the generated feature vectors to train and test a Multi Layer model aimed at predicting AD/CN(ADNI) or AD/CTL(ANMerge).

1) Gene expression branch: The first step in the modeling pipeline involves training a fully connected neural network model specifically on the gene expression data, as shown in Fig. 1 (I) and Fig. 2 (a). This model is designed to classify subjects as either AD or CN based on their gene expression profiles.

Model architecture: The gene expression model is a fully connected neural network with multiple layers, as shown in Fig. 2 (a). The input layer consists of 464 nodes, corresponding to the 464 highly variable genes we selected in Section 2.1. This is followed by several hidden layers with ReLU activation functions, which extract meaningful features from the input data. The output layer consists of two nodes, representing the AD and CN classes, to predict the probability of each class, as shown in Fig. 1 (I).

Training process: The model is trained using a binary cross-entropy loss function and optimized using the Adam optimizer using 30 epochs. Once the model is trained, the features of the final hidden layer are extracted and saved. These features serve as a condensed representation of the gene expression data and are later used in the IG-CVAE model to correlate the generated gene expression feature vector.

2) MRI branch: Next, we train a 3D convolutional neural network (CNN) on the 3D MRI data. This model is designed to classify subjects as AD or CN based on their MRI scans, as shown in Fig. 1 (I) and Fig. 2 (b).

Model architecture: The MRI model is a 3D CNN that processes the input MRI volumes through a series of fully connected convolutional, pooled and convolutional layers, as shown in Fig. 2 (b). The convolutional layers extract spatial

features from the MRI scans, while the fully connected layers combine these features to make the final classification. The output layer, similar to the gene expression model, predicts the probability of each class, as shown in Fig. 1 (I).

Training process: The MRI model is trained using a binary cross-entropy loss function and the Adam optimizer with 10 epochs. The training process includes data augmentation techniques, such as random rotations, normalization, and intensity scaling, to improve the model's generalizability. The features from the final fully connected layer are extracted and saved. These features represent a condensed view of the MRI data and will be used as input to the IG-CVAE model.

3) IG-CVAE: The IG-CVAE model architecture is based on a conditional variational autoencoder (CVAE), which is well-suited for generating data that is conditioned on certain inputs, as shown in Fig. 1 (II) and Fig. 2 (c). In this case, the CVAE generates gene expression data conditioned on 3D MRI scans. The CVAE consists of two main components: an encoder and a decoder. The encoder is a full connected neural network with 3 layers that processes the input MRI feature vector data, extracting the mean and variance of size 128. The encoder outputs these two parameters, which are crucial for modeling the uncertainty and variability inherent in the MRI data. By learning the mean and variance, the encoder allows the model to capture a distribution of possible latent representations rather than a single deterministic point, thereby enabling the generation of diverse and biologically plausible gene expression profiles based on Gaussian distribution [18]. The decoder is a fully connected neural network that takes the latent representation as input and generates the corresponding gene expression feature vector data of size 128. By conditioning the decoder on the MRI-derived latent space, the CVAE learns to generate gene expression profiles that are consistent with the structural brain feature vector data.

C. Components of IG-CVAE loss function

The IG-CVAE model is trained using a combination of loss functions designed to enhance the model's ability to generate accurate and biologically meaningful gene expression data from MRI inputs. These loss functions include the reconstruction loss [18], Kullback-Leibler (KL) divergence [18], and cosine similarity loss [19].

1) Reconstruction loss:: It measures the difference between the generated gene expression features and the real gene expression features [18]. We have used mean absolute error (MAE) and mean square error (MSE) in the IG-CVAE loss to enhance the model reconstruction power and ensure that the generated data closely resembles the real data, capturing the essential characteristics of the gene expression profiles. As we reduce the loss, it train the model to reconstruct gene expression feature vector data as accurately as possible to the actual data, thereby improving the overall fidelity of the generated outputs.

2) KL divergence:: KL divergence is a crucial component that regularizes the latent space of the CVAE. It encourages the latent variables to follow a Gaussian distribution, which helps prevent over-fitting and ensures that the latent representations are smooth and continuous [18]. To control the complexity of the latent space to the unseen data this regulaization is important.

3) Cosine similarity loss:: It guides the model in generating gene expression data that preserves the directional relationships between genes [19]. Measures the cosine of the angle between the feature vectors of the generated and the real gene expression data feature vector, penalizing the model if the generated data deviates from the correct direction in the feature space. Hence this loss is important to ensure that the model is generating data maintaining the biological interactions with the real feature vector data, thereby enhancing the biological relevance of the predictions.

4) IG-CVAE loss:: The overall loss function is a weighted combination of these components, represented by the formula to train the IG-CVAE model:

$$\begin{aligned} IG-CVAELoss = {} & ReconstructionLoss(BCE + MAE) \\ & + 0.01 \times KLdivergence \\ & + 0.001 \times CosineSimilarityLoss \end{aligned} \tag{1}$$

This combination creates a more robust and biologically accurate generative model. The training process involves using 90% of the available gene expression and MRI data for training, while 10% is reserved for testing. The model is optimized using the Adam optimizer with a learning rate of 0.001 and a batch size of 32.

D. Evaluation and Validation

The performance of the IG-CVAE model is evaluated using a comprehensive set of metrics that assess both the accuracy and the biological relevance of the generated gene expression data.

To evaluate the effectiveness of generative models in computational biology and machine learning, several well-established metrics are employed. The Mean Squared Error (MSE) quantifies the average squared differences between generated and real gene expression data, with lower values reflecting closer alignment to real data [20]. Similarly, Mean Absolute Error (MAE) focuses on the absolute deviations between the generated and real feature vector data [21]. The Mean Absolute Percentage Error (MAPE) check for the proportional accuracy of the generated data with the real data, to maintain biological consistency [21]. Cosine Similarity verifies the directional alignment, to maintain the preservation of gene feature vector interaction patterns [19]. Together, these metrics provide a comprehensive framework to assess the alignment of generated data with biological expectations and real-world variability.

III. Results

The performance of the IG-CVAE model was rigorously evaluated using multiple metrics, including MSE, MAE, MAPE, and cosine similarity. For ADNI dataset, as shown in

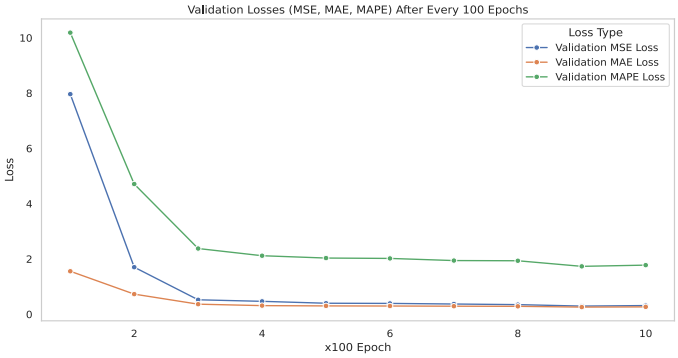

Fig. 3. MAE, MSE, and MAPE Loss with 1000 epochs for IG-CVAE - ADNI Dataset

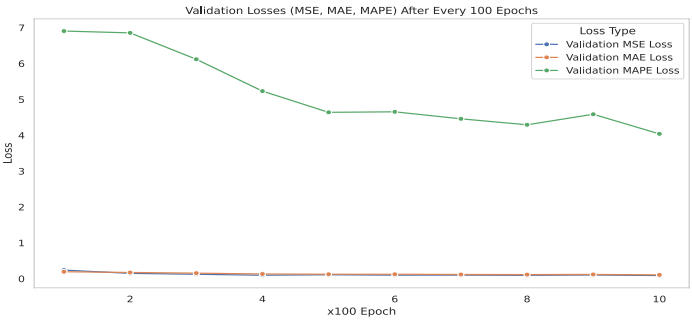

Fig. 4. MAE, MSE, and MAPE Loss with 1000 epochs for IG-CVAE - ANMerge Dataset

TABLE I, the MSE between the generated gene expression data feature vector and the real gene data feature vector was 0.217, indicating a low average squared difference and reflecting the model's accuracy in generating data that closely matches the ground truth. The model achieved a cosine similarity (maintaing the directional relationships) of 99.997% at the 1000 epoch, ensuring the biological integrity of the data. The MAE was recorded at 0.217, suggesting minimal deviation between the generated and actual gene expression values. The MAPE was 1.43, highlighting the precision of the model in generating gene expression data that closely mimics the real data across different magnitudes. As the number of epochs increases, the MSE, MAE, and MAPE loss decreases, and at 1000 epochs, it almost becomes constant, as shown in Fig. 3.

Furthermore, the generated gene expression feature vectors using CVAE model, were used to train an MLP classification model to predict binary outcomes (AD/CN) at 1000 epochs. This step evaluates the utility of the generated features for downstream classification tasks. The MLP model achieved an accuracy of 84.75%, precision of 96.51%, an F1-score of 78.12%, and a recall of 70.54% in the test set, indicating that the generated features effectively capture the patterns required for classification tasks. TABLE II shows different model performance with input as a generated feature vector.

Similarly for ANMerge dataset, as shown in TABLE I, the MSE between the generated gene expression data feature vector and the real gene data feature vector was 0.08. The model achieved a cosine similarity of 99.998% at the 1000 epoch, demonstrating that the generated data preserves the directional relationships between genes. The MAE was recorded at 0.106. The MAPE was 4.038, highlighting the precision of the model in generating gene expression data that closely mimics the real data across different magnitudes. As the number of epochs increases, the MSE, MAE, and MAPE loss decreases, and at 1000 epochs, it almost becomes constant, as shown in Fig. 4.

As shown in TABLE II ANMerge section, the generated gene expression feature vectors were used to predict binary outcomes with different models. The MLP model achieved an accuracy of 96.23%, precision of 95.02%, an F1-score of 97.33%, and a recall of 99.75% on the test set, hence the generated features capture the patterns required for classification tasks.

Together, these metrics collectively indicate that our IG-CVAE model, particularly when enhanced with IG-CVAE loss, is highly effective in generating accurate and biologically relevant gene expression data from MRI features.

The progression of IG-CVAE model performance across different epochs is summarized in Fig. 3, where we are generating gene expression feature vectors of size 128 with MRI 3D data. The results show significant improvement in all metrics as the training progresses.

IV. Discussion

This study presents a novel approach to generating gene expression feature vector data from 3D MRI scans using IG-CVAE model. The results underscore the effectiveness of our method in not only replicating gene expression feature vector data with high accuracy but also in preserving its biological relevance. Notably, we benchmark our model with single modality models to make sure the synthetic data are generated from the validated model. To the best of our knowledge, this approach has never been explored or achieved before to help better understand AD underlying mechanisms based on generative gene expression data from neuroimaging data. Our gene expression model as shown in Fig. 2 (a), trained on feature vectors derived from gene data, predicts AD or CN states with high accuracy while providing insights into feature importance where key genes such as AK2 (Adenylate Kinase 2) and CETN2 (Centrin EF-hand Protein 2), plays a important role to train the model for the predictions, validated by SHAP analysis [21]. Interestingly, it aligns with findings from [22], showcasing the robustness of the model. Our preliminary results have demonstrate the reliability of the synthetic gene expression data in predicting AD. More details will be shared in the future work.

Building on this, we have started to extend our approach to explore correlations between gene feature vectors and specific brain regions using a Grad-CAM-based methodology. While traditional Grad-CAM[23] methods focus on identifying 2D regions critical for class predictions (e.g., RGB images), our approach localizes 3D MRI regions associated with synthetic features or gene symbols. Specifically, we calculate gradients

Epoch	ADNI Dataset				ANMerge Dataset			
	Cosine Similarity	MAE	MSE	MAPE	Cosine Similarity	MAE	MSE	MAPE
100	0.99995	1.52	8.29	9.91	0.99994	0.19	0.24	6.90
300	0.99996	0.247	0.268	1.61	0.99996	0.15	0.12	6.11
500	0.99996	0.23	0.248	1.52	0.99997	0.12	0.11	4.64
800	0.99996	0.23	0.239	1.52	0.99998	0.115	0.09	4.29
1000	0.99997	0.217	0.217	1.43	0.99998	0.106	0.08	4.04

TABLE I

PERFORMANCE METRICS COMPARISON ACROSS EPOCHS FOR GENERATED FEATURE VECTORS FROM MRI 3D DATA AND GENE EXPRESSION FEATURE VECTOR DATA FOR ADNI AND ANMERGE DATASETS.

Model	ADNI Dataset				ANMerge Dataset			
	Accuracy	F1-Score	Precision	Recall	Accuracy	F1-Score	Precision	Recall
Random Forest	0.76	0.52	0.68	0.48	0.93	0.95	0.94	0.97
XGBoost	0.80	0.65	0.96	0.60	0.95	0.97	0.96	0.98
MLP	0.84	0.78	0.96	0.70	0.96	0.97	0.95	0.99

TABLE II

PERFORMANCE METRICS COMPARISON ACROSS DIFFERENT MODELS TO PREDICT AD/CN FOR ADNI DATASET AND AD/CTL FOR ANMERGE DATASET BASED ON GENERATED GENE FEATURE VECTORS.

with respect to the 3D MRI input and leverage a shared latent space (128-dimension) to generate interpretable 3D heatmaps.

This advancement enables us to better understand the biological relevance of brain regions contributing to gene expression variations across various stage of the AD progression. By uncovering the interactions between these modalities and their implications for disease etiology and progression, we aim to promote precision medicine in clinical settings. More uncovering and validation will come in the next months.

V. CONCLUSION

By addressing the pressing challenge of gene expression data scarcity in ADNI and ANMerge datasets, alongside MRI imaging, our research presents a novel framework for improving AD detection and understanding. Through the integration of CVAE with Gaussian Distribution, we successfully generated synthetic gene expression feature vector data from 3D MRI features with predicting stages of AD. This innovative approach bridges critical gaps in data availability between the gene expression data and neuroimaging data, which could enhance the performance of correlation and detection of AD in the patients and its pattern based on gene symbols and MRI specific region. Next, we will extend our pioneering model framework to enhance explainability and generalizability with more experimental and clinical validations.

ACKNOWLEDGMENT

Data used in the preparation of this article were obtained from the Alzheimer's Disease Neuroimaging Initiative (ADNI) database (adni.loni.usc.edu) and ANMerge (syn4988768). As such, the investigators within the ADNI contributed to the design and implementation of ADNI and/or provided data but did not participate in the analysis or writing of this report. A complete listing of ADNI investigators can be found at: (http://adni.loni.usc.edu/wp-content/uploads/how_to_apply/ADNI_Acknowledgement_List.pdf)

REFERENCES

[1] V. Adarsh, G. R. Gangadharan, U. Fiore, and P. Zanetti, "Multimodal classification of alzheimer's disease and mild cognitive impairment using custom mkscddl kernel over cnn with transparent decision-making for explainable diagnosis," *Scientific reports*, vol. 14, Jan. 2024. DOI: 10.1038/s41598-024-52185-2. (visited on 05/29/2024).

[2] A. Nordberg, "Insights into the progression of genetic alzheimer's disease from tau pet," *The Lancet Neurology*, vol. 23, pp. 453–454, May 2024. DOI: 10.1016/s1474-4422(24)00124-8. (visited on 08/30/2024).

[3] L. Li, X. Yu, C. Sheng, *et al.*, "A review of brain imaging biomarker genomics in alzheimer's disease: Implementation and perspectives," *Translational Neurodegeneration*, vol. 11, p. 42, Sep. 2022. DOI: 10.1186/s40035-022-00315-z. [Online]. Available: https://www.ncbi.nlm.nih.gov/pmc/articles/PMC9476275/.

[4] S. Zhang, Y. Zhou, P. Geng, and Q. Lu, "Functional neural networks for high-dimensional genetic data analysis," *IEEE/ACM Transactions on Computational Biology and Bioinformatics*, vol. 21, pp. 383–393, May 2024. DOI: 10.1109/tcbb.2024.3364614. (visited on 08/28/2024).

[5] S. S. M. Elsheikh, E. R. Chimusa, N. J. Mulder, and A. Crimi, "Genome-wide association study of brain connectivity changes for alzheimer's disease," *Scientific Reports*, vol. 10, Jan. 2020. DOI: 10.1038/s41598-020-58291-1. (visited on 11/13/2021).

[6] E. Lin, C.-H. Lin, and H.-Y. Lane, "Deep learning with neuroimaging and genomics in alzheimer's disease," *International Journal of Molecular Sciences*, vol. 22, p. 7911, Jul. 2021. DOI: 10.3390/ijms22157911.

[7] J. Wu, Y. Chen, P. Wang, *et al.*, "Integrating transcriptomics, genomics, and imaging in alzheimer's disease:

A federated model," *Frontiers in Radiology*, vol. 1, Jan. 2022. DOI: 10.3389/fradi.2021.777030. (visited on 08/29/2024).

[8] L. Ibanez, C. Cruchaga, and M. V. Fernández, "Advances in genetic and molecular understanding of alzheimer's disease," *Genes*, vol. 12, p. 1247, Aug. 2021. DOI: 10.3390/genes12081247. (visited on 02/02/2022).

[9] Y. Pan, M. Liu, Y. Xia, and D. Shen, "Disease-image-specific learning for diagnosis-oriented neuroimage synthesis with incomplete multi-modality data," *IEEE Transactions on Pattern Analysis and Machine Intelligence*, 1–1, 2021. DOI: 10.1109/TPAMI.2021.3091214. [Online]. Available: https://ieeexplore.ieee.org/document/9462380 (visited on 06/10/2022).

[10] P. Kodam, R. S. Swaroop, S. S. Pradhan, V. Sivaramakrishnan, and R. Vadrevu, "Integrated multi-omics analysis of alzheimer's disease shows molecular signatures associated with disease progression and potential therapeutic targets," vol. 13, Mar. 2023. DOI: 10.1038/s41598-023-30892-6. (visited on 06/17/2023).

[11] A. K. Agarwal, V. Gupta, P. Brahmbhatt, *et al.*, "Amyloid-related imaging abnormalities in alzheimer disease treated with anti–amyloid- therapy," *Radiographics*, vol. 43, Sep. 2023. DOI: 10.1148/rg.230009.

[12] L. T. Elliott, K. Sharp, F. Alfaro-Almagro, *et al.*, "Genome-wide association studies of brain imaging phenotypes in uk biobank," *Nature*, vol. 562, pp. 210–216, Oct. 2018. DOI: 10.1038/s41586-018-0571-7. (visited on 01/09/2022).

[13] M. Ewers, R. A. Sperling, W. E. Klunk, M. W. Weiner, and H. Hampel, "Neuroimaging markers for the prediction and early diagnosis of alzheimer's disease dementia," *Trends in Neurosciences*, vol. 34, pp. 430–442, Aug. 2011. DOI: 10.1016/j.tins.2011.05.005. [Online]. Available: https://www.ncbi.nlm.nih.gov/pmc/articles/PMC3275347/ (visited on 03/29/2019).

[14] M. A. Hill and S. C. Gammie, "Alzheimer's disease large-scale gene expression portrait identifies exercise as the top theoretical treatment," *Scientific Reports*, vol. 12, p. 17 189, Oct. 2022. DOI: 10.1038/s41598-022-22179-z. [Online]. Available: https://www.nature.com/articles/s41598-022-22179-z#Abs1 (visited on 11/21/2022).

[15] C. Birkenbihl, S. Westwood, L. Shi, *et al.*, "Anmerge: A comprehensive and accessible alzheimer's disease patient-level dataset," *Journal of Alzheimer's Disease*, vol. 79, 423–431, Jan. 2021. DOI: 10.3233/JAD-200948. [Online]. Available: https://content.iospress.com/articles/journal-of-alzheimers-disease/jad200948 (visited on 03/16/2022).

[16] S. Qiu, M. I. Miller, P. S. Joshi, *et al.*, "Multimodal deep learning for alzheimer's disease dementia assessment," *Nature Communications*, vol. 13, p. 3404, Jun. 2022. DOI: 10.1038/s41467-022-31037-5. [Online]. Available: https://www.nature.com/articles/s41467-022-31037-5.

[17] M. E. Ritchie, B. Phipson, D. Wu, *et al.*, "Limma powers differential expression analyses for rna-sequencing and microarray studies," *Nucleic Acids Research*, vol. 43, e47–e47, Jan. 2019. DOI: 10.1093/nar/gkv007.

[18] D. P. Kingma and M. Welling, "Auto-encoding variational bayes," *arXiv (Cornell University)*, Dec. 2013. DOI: 10.48550/arxiv.1312.6114.

[19] G. Koch, R. Zemel, and R. Salakhutdinov, *Siamese neural networks for one-shot image recognition*, 2015. [Online]. Available: https://www.cs.cmu.edu/~rsalakhu/papers/oneshot1.pdf.

[20] J. Zrimec, X. Fu, A. S. Muhammad, *et al.*, "Controlling gene expression with deep generative design of regulatory dna," *Nature Communications*, vol. 13, Aug. 2022. DOI: 10.1038/s41467-022-32818-8. [Online]. Available: https://www.ncbi.nlm.nih.gov/pmc/articles/PMC9427793/ (visited on 01/31/2023).

[21] W. Zhou, Z. Yan, and L. Zhang, "A comparative study of 11 non-linear regression models highlighting autoencoder, dbn, and svr, enhanced by shap importance analysis in soybean branching prediction," *Scientific Reports*, vol. 14, p. 5905, Mar. 2024. DOI: 10.1038/s41598-024-55243-x. [Online]. Available: https://www.nature.com/articles/s41598-024-55243-x (visited on 04/28/2024).

[22] N. Voyle, A. Keohane, S. Newhouse, *et al.*, "A pathway based classification method for analyzing gene expression for alzheimer's disease diagnosis," *Journal of Alzheimer's Disease*, vol. 49, 659–669, Jan. 2016. DOI: 10.3233/JAD-150440. [Online]. Available: https://content.iospress.com/articles/journal-of-alzheimers-disease/jad150440 (visited on 04/13/2023).

[23] R. R. Selvaraju, M. Cogswell, A. Das, R. Vedantam, D. Parikh, and D. Batra, "Grad-cam: Visual explanations from deep networks via gradient-based localization," *International Journal of Computer Vision*, vol. 128, 336–359, Feb. 2020. DOI: 10.1007/s11263-019-01228-7.